Original Article

Association between features of intraoperative ultrasound and magnetic resonance imaging in the diagnosis of dysembryoplastic neuroepithelial tumor

Linggang Cheng, Lin Zhang, Lu Yin, Wei Zhang, Wen He

Department of Ultrasound, Beijing Tiantan Hospital, Capital Medical University, Beijing, China

Contributions: (I) Conception and design: L Cheng, W He; (II) Administrative support: L Zhang; (III) Provision of study materials or patients: L Yin; (IV) Collection and assembly of data: L Cheng; (V) Data analysis and interpretation: W Zhang; (VI) Manuscript writing: All authors; (VII) Final approval of manuscript: All authors.

Correspondence to: Wen He. Department of Ultrasound, Beijing Tiantan Hospital, Capital Medical University, 119 South Fourth Ring West Road, Fengtai District, Beijing 100160, China. Email: hewen@bjtth.org.

Background: To analyze the characteristics of images from intraoperative ultrasound (IoUS) and preoperative magnetic resonance imaging (MRI) and their relationship with pathological components of dysembryoplastic neuroepithelial tumor (DNT) and to discuss the role of IoUS in detecting tumor residues.

Methods: The clinical and image data of 24 patients with postoperative pathology-confirmed DNT were analyzed retrospectively. Baseline characteristics, imaging features, and intraoperative residues were recorded for further analysis. Cohen's kappa consistency evaluation was performed on the echo and signal characteristics of the lesions.

Results: Cohen's kappa coefficient between the echo and signal of the lesion was 0.832. The characteristics of IoUS were gyrus or mass hyperechoic solid nodules located under the cortex, insufficient blood flow signals, and clear boundaries, in addition to mixed cystic and solid echo nodules. The solid part of the lesion consisted of pathologically nodular specific glioneuronal element (SGE) or was combined with glial nodules and focal cortical dysplasia (FCD), which was characterized by a high echo or long T1 long T2 signal and uniform or uneven distribution. The cystic part consisted of a mucinous matrix, showing echoless or long T1 long T2 on fluid attenuated inversion recovery (FLAIR), which was higher than that in cerebrospinal fluid but lower than that in the cerebral cortex. The residual lesion discovered using IoUS was confirmed with postoperative MRI.

Conclusions: The IoUS characteristics of DNT are strongly consistent with MRI, and its imaging features are related to pathological components. IoUS can assist the operator to judge the mode and scope of tumor resection, detect residual tumor, and improve the rate of total tumor resection.

Keywords: Intraoperative ultrasound (IoUS); dysembryoplastic neuroepithelial tumor (DNT); magnetic resonance imaging (MRI)

Submitted Jun 26, 2022. Accepted for publication Nov 27, 2022. Published online Dec 08, 2022.
doi: 10.21037/qims-22-677
View this article at: https://dx.doi.org/10.21037/qims-22-677

Introduction

Dysembryoplastic neuroepithelial tumor (DNT) is relatively rare and is classified as a World Health Organization (WHO) grade I benign tumor. It mainly occurs in the temporal and frontal lobes. Other rare sites of DNT include the septum pellucidum, cauda equina, thalamus, and cerebellum (1,2). Morbidity is high in children and young people and is lower in females than in males. Its incidence peaks from 10 to 14 years of age (3). The tumor exhibits slow growth, and the lesions are mostly confined to the cerebral cortex and partly invade the white matter of the subcortical brain. Patients often seek medical treatment because of drug-resistant epilepsy. Complete surgical resection and extended resection of lesions are the main treatment methods. Most patients achieve long-term remission without radiotherapy and chemotherapy (4-6).

Magnetic resonance imaging (MRI) is a suitable imaging method for preoperative diagnosis of DNT. However, neurosurgeons need to locate the focus in real-time during the operation to show the residual tumor and to clearly visualize the position of the tumor in relation to the surrounding brain tissue and large blood vessels. This requires real-time display during the operation using imaging technology.

The application of intraoperative ultrasound (IoUS) solves these problems. IoUS was first used in neurosurgery in 1961. After more than 60 years of development, it has been gradually accepted and recognized by surgeons and researchers. Its function is to evaluate, quantify, and correct brain drift before surgery; adjust the surgical path real-time; detect bleeding and hematoma during the operation; and identify residual tumor after the operation without radiation. At the same time, it can minimize the impact of the surgical process (7,8). Based on a summary of the IoUS characteristics of DNT, we found that it has specific ultrasonic image characteristics, which can improve the user's understanding of the tumor, estimate the resection scope and operation method of the lesion, and identify the residual condition to achieve a better treatment outcome.

Up to now, there have been few studies on the use of IoUS in DNT. We reviewed preoperative MRI and IoUS images of patients with DNT in our hospital, analyzed the characteristics and correlation between IoUS and MRI, summarized the relationship between IoUS and MRI images, and discussed the role of IoUS in reducing residual tumor.

Methods

The study was conducted in accordance with the Declaration of Helsinki (as revised in 2013). This prospective study was approved by the Institutional Review Board of the Beijing Tiantan Hospital (No. KY2018-097-02), and informed consent was provided by all patients.

Sample

Patients who underwent DNT resection in Beijing Tiantan Hospital from 2012 to 2020 were included. The exclusion criteria were the presence of multiple intracranial lesions, tumor recurrence, and other intracranial lesions. All selected patients signed preoperative informed consent and underwent IoUS examination.

IoUS examinations

A Hitachi Noblus scanner (Hitachi, Tokyo, Japan) with a C42 convex array probe (frequency: 3–12 MHz) was used to acquire B-mode images. The probe surface was disinfected, couplant was applied, the probe was wrapped in a sterile probe sleeve, normal saline was used as the medium, the probe was placed on the dura mater or brain surface for scanning, the scanning depth was 10–15 cm, and the probe was then adjusted appropriately according to the location and size of the focus. The image was adjusted to optimize the display of lesions. The focus was located after the bone flap removal before the dura mater was opened. After the dura mater was cut off, the parameters of the focus were measured; during the operation, the resection of the focus was observed occasionally to check if the brain tissue around the focus was normal; after the operation, the residual lesions were explored, and B-mode images were collected. The coronal, sagittal, and transverse images of the focus were obtained. The ultrasound image obtained was consistent with the corresponding section of the MRI image as far as possible, such as the ventricle or brain stem, which can be identified easily in ultrasound and MRI images, and which were used as anatomical landmarks. The location, size, shape, boundary, echo, blood supply, edema, and location in relation to the surrounding brain tissue were recorded. The maximum diameter of the focus was measured at the maximum section of the focus, and then the images were exported for analysis. The IoUS images were analyzed independently by 2 ultrasonographers with more

Table 1 Clinical information of patients, tumor characteristics, and results of focal resection

Characteristics	Total n=24
Age (years), range (mean ± SD)	2–56 (15.04±13.61)
Sex	
Male	16
Female	8
Tumor size (mm), range (mean ± SD)	19–52 (34.73–9.52)
Tumor location	
Temporal lobe	9
Parietal lobe	5
Parietal and frontal lobes	1
Frontal lobe	7
Occipital lobes	2
Alteration of the surrounding tissues	
Compressed	7
Normal	17
Syndrome	
Epilepsy	17
Dizziness	3
Blurred vision	1
Leg ache	1
Asymptomatic	2
Focal resection	
Total resection	19
Subtotal resection	5

SD, standard deviation.

than 5 years of experience in IoUS, using a double-blind method. In the event of inconsistent results, the ultrasound chief physician was asked to assist with the image analysis.

MRI examinations

A GE Signa 1.5T (GE Healthcare, Chicago, IL, USA) or GE Discovery MR750 3.0T (GE Healthcare), Siemens Magnetom trio 3.0T (Siemens, Munich, Germany) or Siemens Verio 3.0T superconducting magnetic resonance imager and 8-channel head coil (Siemens) were used to perform conventional sequence of transverse axial, sagittal, and coronal T1-weighted image (T1WI) (TR 450–500 ms, TE 14–20 ms), transverse axial T2-weighted image (T2WI) (TR 4,000–5,000 ms, TE 120–140 ms), inversion recovery sequence fluid attenuated inversion recovery (FLAIR), and diffusion-weighted imaging (DWI). All patients undergoing enhanced scanning provided written informed consent and were injected with gadolinium tetroxide (GD-DTPA) through a peripheral vein, and transverse, sagittal, and coronal enhanced scans were performed at a dose of 0.1 mmol/kg. The MRI evaluation included the location, size, shape, boundary, signal, enhancement, peripheral edema, and brain tissue compression of the lesion. In some cases, FLAIR and DWI were added for corresponding sequence evaluation. The maximum diameter of the lesion was measured at the maximum section of the lesion. The above contents were performed by a senior neuroradiologist independently before surgery. The MRI images were analyzed independently by 2 radiologists with more than 5 years of experience, using a double-blind method. In the event of inconsistent results, the radiologist chief physician was asked to assist with image analysis.

Statistical analysis

The statistical software SPSS Version 22.0 (IBM Corp., Armonk, NY, USA) was used for statistical analysis. All measurement data were expressed as mean ± standard deviation or median and quartile. The IoUS features of the enrolled patients were divided into 3 groups: (I) uneven high, (II) uniform high, and (III) cystic solid; The MRI image features of the enrolled patients were divided into 3 groups: (I) uneven long T1WI long T2WI, (II) long T1WI long T2WI, and (III) cystic solid. Cohen's kappa consistency evaluation was performed on the image features of 2 images of the lesions. Differences were considered statistically significant when $P<0.001$. The strength of the associations was assessed using Cohen's kappa coefficient.

Results

A total of 24 patients were included in the final study sample. *Table 1* summarizes the sample's clinical features and the surgical resection characteristics of the lesions. We performed IoUS in 24 patients, including 16 males and 8 females, aged 2 to 56 years, with an average age of 15.04±13.61 years. A total of 17 patients were treated for symptomatic epilepsy, 3 for dizziness, 1 for blurred vision, 1 for paroxysmal left leg pain, and 2 asymptomatic patients were identified accidentally during a physical examination.

Table 2 IoUS features of the 24 patients with DNT

Characteristics	Total n=24
Border	
Clear	21
Unclear	3
Morphology	
Cloudy (lamellar)	17
Wedge-shape	3
Gyrus-shape	1
Irregular	3
Echo	
Uneven high echo	16
Uniform high echo	6
Cystic solid	2
Peripheral edema	0
Occupying effects	
Yes	7
No	17

IoUS, intraoperative ultrasound; DNT, dysembryoplastic neuroepithelial tumor.

All 24 patients were operated on successfully. As confirmed by IoUS, 19 lesions were completely resected under the microscope, and 5 were nearly resected. Among the 5 patients with near total resections, 2 patients were retained, because the residual lesions detected by IoUS showed no significant differences compared with the surrounding normal brain tissue under the microscope, and another 3 underwent residual lesion resection under the guidance of IoUS. All patients were instructed to continue antiepileptic treatment after the operation. They were followed up to December 2020. Among them, 1 patient had a postoperative epilepsy remission 2 years later, followed by tumor recurrence and re-operation. The remaining 23 patients showed a significant or complete remission of seizures and other symptoms after treatment. No deaths occurred.

IoUS examinations

The IoUS features of DNT are shown in *Table 2*. The shape of the lesions was regular, of which 17 were lumpy (flaky) and involved multiple adjacent gyri, in 1 patient a gyrus was affected (only one gyrus was involved), the lesions of 3 patients were wedge-shaped, and those of 3 patients were irregular; the boundary between lesions and surrounding tissues was unclear in 3 patients, and most lesions had a clear boundary. There were no obvious signs of edema in the surrounding brain tissue. A total of 7 patients had local deformation of the ventricle, among whom 3 had slight expansion due to traction of the focus, and 4 had slight compression of the ventricle. The echoes of tumor of 22 patients were higher than those of the brain parenchyma, 2 showed mixed and solid cysts, and the solid parts were also higher than brain parenchyma in the echo. The echo of lesions was uneven in 16 patients and uniform in 8 patients (*Figure 1*). No hyperechoic calcification was found in the lesions. Linear hyperechoic separation was seen in most lesions (19 patients). The blood flow of the lesions indicated grade 0 or 1. Strip or dot blood flow signals could be seen in the center and around the lesions.

MRI examinations

A total of 22 patients of preoperative MRI data were included. Among them, 16 patients showed a mass (slice) shape, 2 showed a beaded (strip shaped), 1 a gyrus shape, 1 a wedge shape, and 2 exhibited irregular shapes. The boundary between lesions and surrounding tissues was clear in 19 patients and unclear in 3 patients. No edema was found around the lesions. There were 7 patients with local ventricle deformation consistent with the IoUS. The lesions showed long T1WI long T2WI signals, of which 18 patients showed uneven signals, and 2 patients exhibited multiple cystic changes; FLAIR images of 10 patients showed uneven high signals; among the 14 patients with apparent diffusion coefficient (ADC)/DWI sequence, 3 had equal DWI signals, 11 exhibited low DWI signals with high ADC, and 3 showed no limited diffusion in the lesions; and, finally, in 7 of 22 patients, enhancement was found with uneven and partial enhancement (*Table 3*). Normal sulcus could be seen in the lesions close to the cerebral cortex and involving the growth of adjacent gyri, with low signals on T1WI and high signals on T2WI.

Correlation between IoUS echo and MRI signal

Cohen's kappa consistency test was performed on the IoUS echo characteristics of 24 patients with DNT lesions and the MRI signal characteristics of 22 patients. The

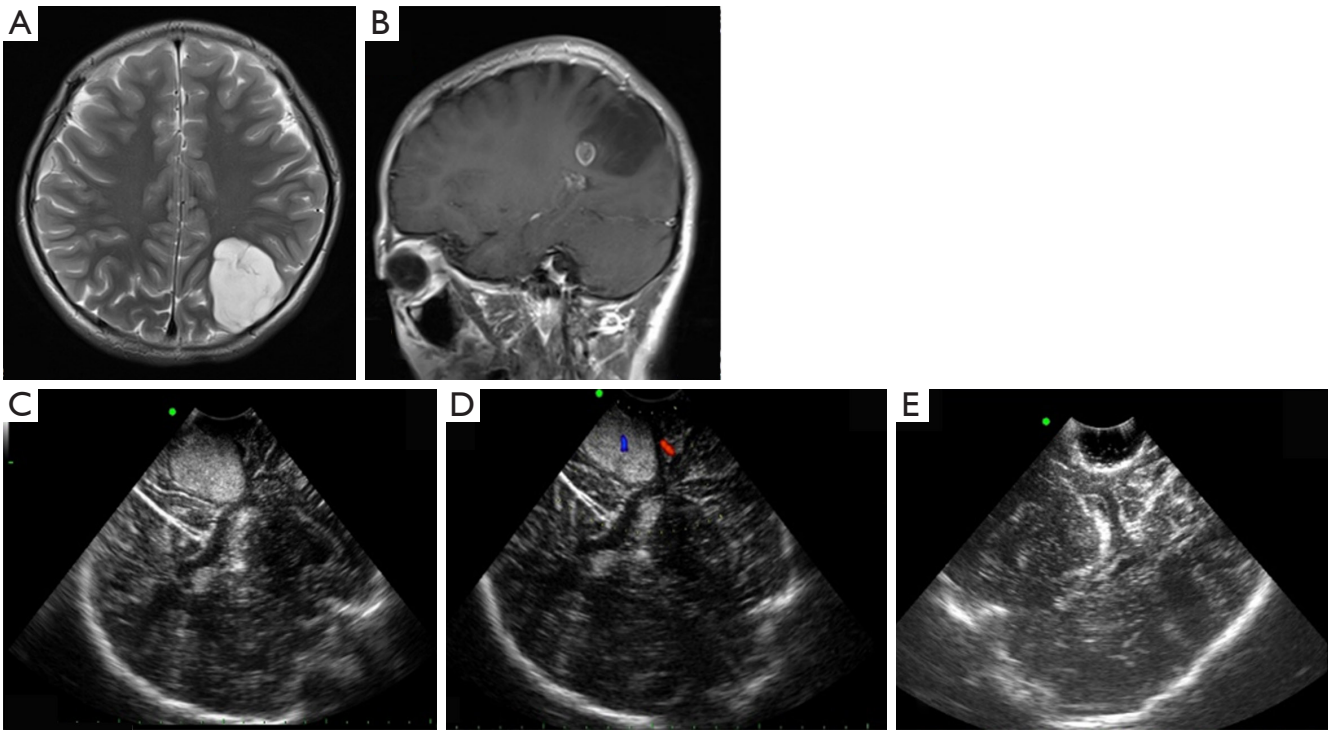

Figure 1 Female, 11 years old. (A,B) Preoperative MRI T1 sagittal and T2 axial images. The lesion is located in the left parietal lobe, showing patchy long T1 and long T2 with a clear boundary Small circular enhancement in the front of the lesion can be seen on enhanced scanning. (C) IoUS shows that the lesion was located on the left side behind the corpus callosum, with a uniform, hyperechoic mass with a clear boundary. (D) Color Doppler flow imaging showed that short-strip blood flow signal can be seen in the lesion. (E) The lesion was completely removed without residue. MRI, magnetic resonance imaging; IoUS, intraoperative ultrasound.

results showed that 12 patients exhibited uneven long T1WI long T2WI signals when IoUS showed uneven hyperechoic; 6 patients showed uniform long T1WI long T2WI signals when IoUS indicated uniform hyperechoic signals; 2 patients exhibited cystic and solid lesions on both IoUS and MRI; 1 showed uniform hyperechoic, and MRI showed uneven long T1WI long T2WI signals; and, finally, 1 showed uneven hyperechoic and uniform long T1WI and long T2WI signals. In general, the IoUS echo characteristics of DNT lesions were consistent with MRI signals, and Cohen's kappa coefficient was 0.832, $P<0.001$.

Discussion

The IoUS of DNT is characterized by gyrus-like or mass hyperechoic solid nodules starting from the subcortical brain, with strong echo linear separation; most have clear boundaries, the mild compression and displacement of the lateral ventricle can be seen if the tumor has a larger size and is growing close to the ventricle, and short strip blood flow signals can be seen around and inside the tumor. The tumor can also be manifested as cystic solid mixed echo nodules, which can be hyperechoic in the solid part and echoless in the cystic part. The solid parts can be nodular specific glial neurons (SGE) and exhibit glial nodules and focal cortical dysplasia (FCD) showing hyperechoic and long T1WI long T2WI signals with uniform or uneven distribution; the cystic part corresponds to the mucinous matrix histologically, showing echoless or long T1WI long T2WI; and the signal on FLAIR is higher than that in the cerebrospinal fluid but lower than that in cerebral cortex. The lesions were linearly separated and hyperechoic on IoUS. On MRI, there were short T1WI short T2WI signals, similar to cortical signals. There was no obvious edema around the focus on IoUS and MRI, but this may have been due to a space-occupying effect. The typical pathological feature of DNT is that the SGE is distributed like single or multiple fusion nodules. This structure consists of oligodendrocyte-like cells (OLC), neurons, and astrocytes. Obvious microcysts in the tumor

Table 3 MRI features of 22 patients with DNT

Characteristics	Total n=22
Border	
Clear	19
Unclear	3
Morphology	
Cloudy (lamellar)	16
Strip (beaded)	2
Wedge-shaped	1
Gyrus-shaped	1
Irregular	2
Signal	
Uniform long T1 long T2	7
Uneven long T1 long T2	13
Cystic solid	2
Enhancement	
Yes	7
No	15
Peripheral edema	0
Occupying effects	
Yes	7
No	15

MRI, magnetic resonance imaging; DNT, dysembryoplastic neuroepithelial tumor.

and a thin basophilic myxoid matrix in the capsule can be seen, including a single neuron scattering (9). OLCs are arranged perpendicular to the cortex, filled with mucoid matrix between cells, or arranged in daisy clusters around capillaries in mucus rich areas, or in nodules between microcapsules (10). The presence of microcysts causes the lesions to be hyperechoic on IoUS with long T1WI long T2WI signals on MRI, that is, they exhibit a so-called pseudocystic structure and a mixed, slightly high signal on FLAIR; the uneven echo or signal of the lesion may be caused by the uneven distribution of SGE and other components in the lesion; when the tumor contains mucinous lake, the signal on T2WI is higher than that in the solid area, DWI shows low signal, and FLAIR is higher than in the cerebrospinal fluid but lower than in the cerebral cortex. Fernandez *et al.* (11) believe that these separations are formed by normal brain sulci and reflect the boundary between the DNT nodular structure and normal cortex and the dense cell area (glial nodule) and loose area (SGE). According to the composition, cell arrangement, and distribution of DNT, it can be divided into a simple type, complex type, and non-special type (12) The simple type only contains SGE, the complex type also contains glial nodules similar to astrocytoma and oligodendroglioma and FCD. The non-special type refers to typical DNT changes in the image, and the clinical characteristics are also consistent with DNT, but the glial cells have no special morphological characteristics on pathological examination, which means they cannot be distinguished from gliomas. Therefore, the existence and classification of this type are controversial (9,13).

MRI is the main imaging method for the diagnosis of DNT. MRI features are as follows: (I) the morphology is nodular or polycystic, and can be triangular or fan-shaped; (II) low or slightly low signal on T1WI, high or slightly high signal on T2WI, high signal on T2 FLAIR lesion edge, and low signal on DWI; and (III) there is no edema or space-occupying effect around the lesion, most lesions are not enhanced, and a few exhibit nodular quasi circular enhancement. Pathologically, they are considered glial nodules, which are usually located around the lesion (14-16). The above description is basically consistent with the signal characteristics of this patient group except for space-occupying effects. Daumas-Duport and Varlet (13) concluded that the diagnosis of DNT can be considered if the following conditions are met: (I) partial seizures, secondary, or without generalized tonic and clonic seizures, and onset before the age of 20; (II) there is no progressive neurological deficit or congenital defect; (III) they are mainly supratentorial lesions, and MRI shows a clear cerebral cortex; and (IV) CT and MRI show no space-occupying effect and no peritumoral edema. IoUS plays an important role in localizing the tumor, clarifying the relationship between blood vessels around the tumor and brain tissue, and assisting the operator to assess the approach and explore the residual tumor. Del Bene *et al.* (15) pointed out that the application of B-ultrasound real-time guidance in the resection of low-grade gliomas can achieve better clinical results, significantly shorten the operation time, and improve the quality of life of patients. In this group of patients, 5 patients' residual lesions were found using IoUS, and 3 patients underwent residual tumor re-resection under the guidance of ultrasound, which improved the total resection rate. In 1 of 2 patients

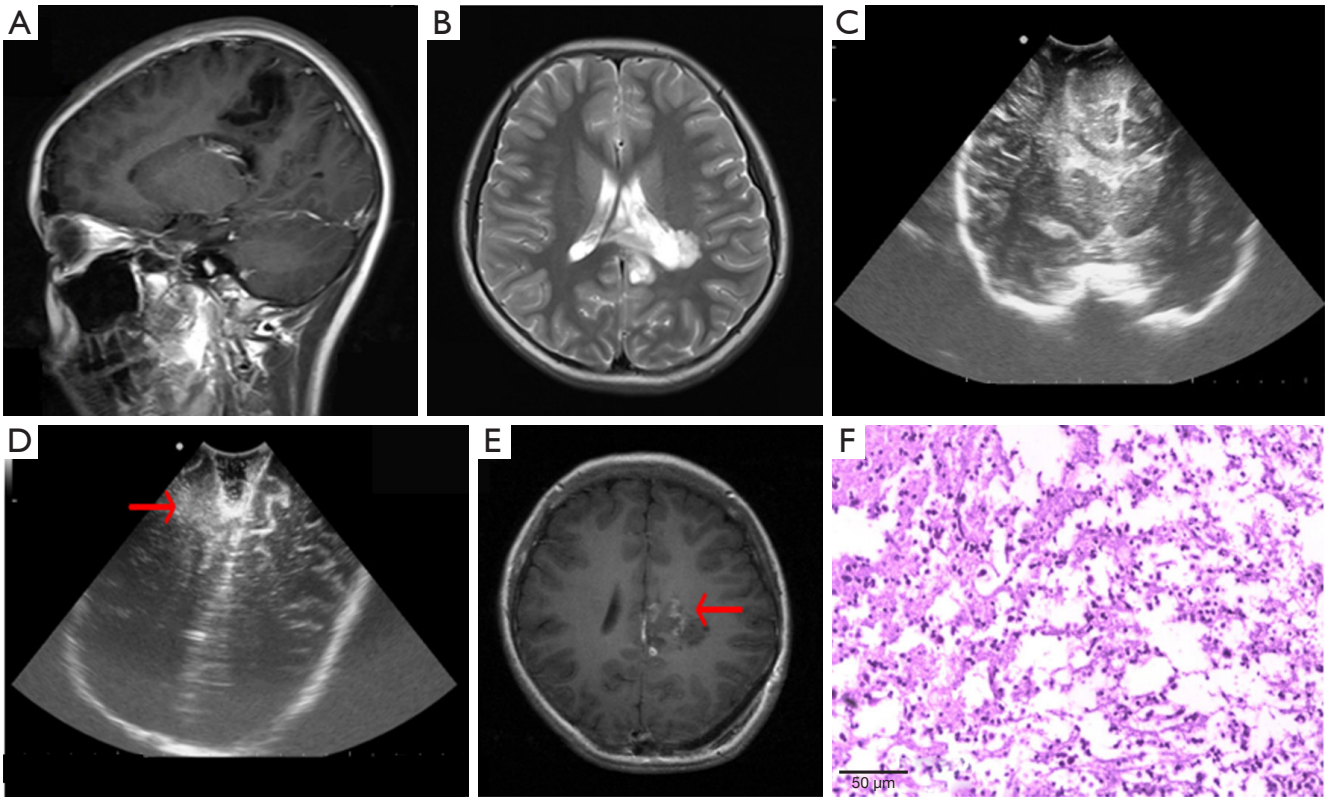

Figure 2 Female, 11 years old. (A,B) Preoperative MRI T1 sagittal and T2 transverse axial images. The lesion is located near the left frontoparietal midline, cingulate gyrus, and lateral ventricle, with a mass shape and long T1 and long T2 signals with clear boundaries. (C) IoUS detected a patchy uneven, slightly hyperechoic lesion at the same position with unclear boundary. (D) The residual tumor around the operation cavity was detected using postoperative ultrasound (red arrow). (E) Postoperative MRI confirmed residual lesions (red arrow) and linear enhancement at the edge of the lesions. (F) Intraoperative pathology showed floating neurons in the area of the tumor cells (HE, ×40), which was consistent with DNT. MRI, magnetic resonance imaging; IoUS, intraoperative ultrasound; DNT, dysembryoplastic neuroepithelial tumor.

with residual lesions, IoUS showed a patchy, slightly hyperechoic area around the operation cavity, which was significantly different from normal brain parenchyma, but there was no significant difference compared with the surrounding normal brain tissue under microscope, and as such the operator retained it. According to the results of postoperative enhanced MRI, abnormal signals with slight enhancement were found in the residual areas indicated using prior ultrasound, indicating that IoUS can accurately detect the residual tumor (*Figure 2*).

Conclusions

IoUS features of DNT involve the cerebral cortex, including regular shape, gyrus, and mass or an oval shape, growing parallel to the gyrus, with a clear boundary and an internal echo that is generally higher than that of the brain parenchyma, and uniform or uneven and linear strong echo separation, which can be seen in the interior with point or strip blood flow. IoUS echo characteristics are highly consistent with the MRI signals and specific. Combined with IoUS's unique pathological and immunohistochemical characteristics, the diagnostic accuracy can be improved. IoUS can help to assess the location and scope of the tumor and the residual tumor during the operation, assist the operator to determine the surgical approach, avoid the large blood vessels around the tumor, and facilitate a total resection of the focus.

Limitations

The deficiency of this study is that this is only a preliminary

study of IoUS of DNT, calcification and bleeding were not assessed, and contrast-enhanced ultrasound and shear wave elastography were not used in this study. Therefore, the IoUS data of the tumor are incomplete, and consequently, there are some inevitable gaps in the assessment of postoperative tumor residue.

The interoperator variability is also known to affect the quality of image and interpretation of IoUS, and as suggested by Ganau *et al.* (12), there should be internationally recognized standards for clinicians and surgeons regarding the use of IoUS. Such international standards would potentially reduce heterogeneity and ensure adherence to best practice (17). Therefore, the summary of IoUS data of these tumors is incomplete, and there are still some inevitable gaps in assessing postoperative tumor residuals.

Acknowledgments

We gratefully thank all patients for their participation in this study.
Funding: This work was supported by the National Natural Science Foundation of China (No. 81730050) and the Cultivation Project of the Beijing Municipal Administration of Hospitals (No. px2018021).

Footnote

Conflicts of Interest: All authors completed the ICMJE uniform disclosure form (available at https://qims.amegroups.com/article/view/10.21037/qims-22-677/coif). The authors have no conflicts of interest to declare.

Ethical Statement: The authors are accountable for all aspects of the work in ensuring that questions related to the accuracy or integrity of any part of the work are appropriately investigated and resolved. The study was conducted in accordance with the Declaration of Helsinki (as revised in 2013). This prospective study was approved by the Institutional Review Board of the Beijing Tiantan Hospital (No. KY2018-097-02), and informed consent was provided by all patients.

References

1. Wen PY, Huse JT. 2016 World Health Organization Classification of Central Nervous System Tumors. Continuum (Minneap Minn) 2017;23:1531-47.
2. Gessi M, Hattingen E, Dörner E, Goschzik T, Dreschmann V, Waha A, Pietsch T. Dysembryoplastic Neuroepithelial Tumor of the Septum Pellucidum and the Supratentorial Midline: Histopathologic, Neuroradiologic, and Molecular Features of 7 Cases. Am J Surg Pathol 2016;40:806-11.
3. Nguyen HS, Doan N, Gelsomino M, Shabani S. Dysembryoplastic Neuroectodermal Tumor: An Analysis from the Surveillance, Epidemiology, and End Results Program, 2004-2013. World Neurosurg 2017;103:380-5.
4. Lee J, Lee BL, Joo EY, Seo DW, Hong SB, Hong SC, Suh YL, Lee M. Dysembryoplastic neuroepithelial tumors in pediatric patients. Brain Dev 2009;31:671-81.
5. Aronica E, Leenstra S, van Veelen CW, van Rijen PC, Hulsebos TJ, Tersmette AC, Yankaya B, Troost D. Glioneuronal tumors and medically intractable epilepsy: a clinical study with long-term follow-up of seizure outcome after surgery. Epilepsy Res 2001;43:179-91.
6. Englot DJ, Han SJ, Berger MS, Barbaro NM, Chang EF. Extent of surgical resection predicts seizure freedom in low-grade temporal lobe brain tumors. Neurosurgery 2012;70:921-8; discussion 928.
7. Cepeda S, Barrena C, Arrese I, Fernandez-Pérez G, Sarabia R. Intraoperative Ultrasonographic Elastography: A Semi-Quantitative Analysis of Brain Tumor Elasticity Patterns and Peritumoral Region. World Neurosurg 2020;135:e258-70.
8. Gerard IJ, Kersten-Oertel M, Hall JA, Sirhan D, Collins DL. Brain Shift in Neuronavigation of Brain Tumors: An Updated Review of Intra-Operative Ultrasound Applications. Front Oncol 2021;10:618837.
9. Campos AR, Clusmann H, von Lehe M, Niehusmann P, Becker AJ, Schramm J, Urbach H. Simple and complex dysembryoplastic neuroepithelial tumors (DNT) variants: clinical profile, MRI, and histopathology. Neuroradiology 2009;51:433-43.
10. Llaguno-Munive M, León-Zetina S, Vazquez-Lopez I, Ramos-Godinez MDP, Medina LA, Garcia-Lopez

P. Mifepristone as a Potential Therapy to Reduce Angiogenesis and P-Glycoprotein Associated With Glioblastoma Resistance to Temozolomide. Front Oncol 2020;10:581814.
11. Fernandez C, Girard N, Paz Paredes A, Bouvier-Labit C, Lena G, Figarella-Branger D. The usefulness of MR imaging in the diagnosis of dysembryoplastic neuroepithelial tumor in children: a study of 14 cases. AJNR Am J Neuroradiol 2003;24:829-34.
12. Ganau M, Ligarotti GK, Apostolopoulos V. Real-time intraoperative ultrasound in brain surgery: neuronavigation and use of contrast-enhanced image fusion. Quant Imaging Med Surg 2019;9:350-8.
13. Daumas-Duport C, Varlet P. Dysembryoplastic neuroepithelial tumors. Rev Neurol (Paris) 2003;159:622-36.
14. Bal J, Camp SJ, Nandi D. The use of ultrasound in intracranial tumor surgery. Acta Neurochir (Wien) 2016;158:1179-85.
15. Del Bene M, Perin A, Casali C, Legnani F, Saladino A, Mattei L, Vetrano IG, Saini M, DiMeco F, Prada F. Advanced Ultrasound Imaging in Glioma Surgery: Beyond Gray-Scale B-mode. Front Oncol 2018;8:576.
16. Yin L, Cheng L, Wang F, Zhu X, Hua Y, He W. Application of intraoperative B-mode ultrasound and shear wave elastography for glioma grading. Quant Imaging Med Surg 2021;11:2733-43.
17. Ganau M, Syrmos N, Martin AR, Jiang F, Fehlings MG. Intraoperative ultrasound in spine surgery: history, current applications, future developments. Quant Imaging Med Surg 2018;8:261-7.

Cite this article as: Cheng L, Zhang L, Yin L, Zhang W, He W. Association between features of intraoperative ultrasound and magnetic resonance imaging in the diagnosis of dysembryoplastic neuroepithelial tumor. Quant Imaging Med Surg 2023;13(2):645-653. doi: 10.21037/qims-22-677

